DEPARTMENT OF DEFENCE
DEFENCE SCIENCE & TECHNOLOGY ORGANISATION
DSTO

DSTO

SensorVision Radiometric Equations Version 2.2

Ninh Duong and
Michael Wegener

DSTO-TN-0193

SensorVision Radiometric Equations Version 2.2

Ninh Duong and Michael Wegener

Weapons Systems Division
Aeronautical and Maritime Research Laboratory

DSTO-TN-0193

ABSTRACT

This technical note describes the radiometric equations employed by an IR scene generation COTS software package called SensorVision. The components of the radiometric equations used to compute the radiance quantities of an IR scene are discussed in detail and assumptions used in the derivation of these equations are identified. The focus of this technical note is to highlight possible sources of errors in an IR scene generated by SensorVision.

RELEASE LIMITATION

Approved for public release

DEPARTMENT OF DEFENCE
DEFENCE SCIENCE & TECHNOLOGY ORGANISATION
DSTO

Published by

DSTO Aeronautical and Maritime Research Laboratory
PO Box 4331
Melbourne Victoria 3001 Australia

Telephone: (03) 9626 7000
Fax: (03) 9626 7999

AR-010-833
February 1999

APPROVED FOR PUBLIC RELEASE

SensorVision Radiometric Equations
Version 2.2

Executive Summary

SensorVision is a commercial-off-the-shelf (COTS) software package that is intended to be used in the Systems Simulation Centre at DSTO for infrared (IR) scene generation in hardware in the loop (HIL) testing of imaging IR systems. Before SensorVision can be applied to the intended application, there is a need to verify and validate the SensorVision package to ensure the generated scenes are sufficiently accurate for HIL simulations. The contents of this technical note constitute the initial phase of the verification and validation procedure, and that is to acquire an understanding of the radiometric equations employed by SensorVision.

Contents

List of Symbols

β	Attenuation constant parameter
γ	Angle between surface normal and unit vector $\hat{s}$
φ	Normalised spectral response of sensor
λ	Wavelength
χ	Cosine of angle between surface normal and unit vector $\hat{s}$
(θ,ϕ)	Elevation and azimuth angle of radiation to surface
ρ	Diffuse reflection coefficient of surface
ρ_h	Hemispherical reflectance of surface
τ	Atmospheric transmission coefficient
Ω	Solid angle
$A_{sun/moon}$	Projected area of the solar or lunar disk
BG	Accumulation buffer gain
BW	Angular bandwidth of specular lobe
c_1	Radiation constant (3.7418×10^8 $Wm^{-2}\mu m^4$)
c_2	Radiation constant (1.438769×10^4 μmK)
DC	Accumulation buffer offset
E	Irradiance
f_s	Fraction of radiation reflected specularly
f_{sl}	Function giving angular dependence of specularly reflected radiation
G	Gain control multiplier
$\hat{i}$	Direction unit vector from surface to sensor
L	Radiance
$L_{ambient}$	Skyshine radiance incident on a surface
L_{bb}	Blackbody radiance emitted from a surface
L_{direct}	Solar/lunar radiance incident on a surface
$L_{observer}$	Total in-band radiance detected by a sensor
L_{path}	Atmospheric path radiance for the line of sight path between a surface and a sensor
$L_{skyshine}$	In-band radiance detected by a sensor due to reflected skyshine or ambient radiance
$L_{solar/lunar}$	In-band radiance detected by a sensor due to solar or lunar reflections

$L_{\substack{solar\,/\,lunar \\ diffuse}}$	In-band radiance detected by a sensor due to solar/lunar diffuse reflections
$L_{\substack{solar\,/\,lunar \\ specular}}$	In-band radiance detected by a sensor due to solar/lunar specular reflections
$L_{sun\,/\,moon}$	Radiance of the sun or moon
L_{SVpath}	In-band radiance detected by a sensor due to atmospheric emissions and forward scattering in the path between a source and the sensor
$L_{thermal}$	In-band radiance detected by a sensor due to thermal emissions
M	Exitance
N	Number of colour bits
n	Pixel value
$\hat{n}$	Surface normal unit vector
N_s	Specular reflection normalisation factor
r	Line of sight range
$\hat{r}$	Direction unit vector from surface to source
R_i	Distance between reflecting surface and solar/lunar disk
$\hat{s}$	Normalised vector summation of $\hat{i}$ and $\hat{r}$
shininess	Parameter defined by angular bandwidth of specular lobe
T	Temperature of body

Abbreviations

API	Application Programming Interface
BW	BandWidth
cbits	colour **bits**
COTS	Commercial Off The Shelf
DoD	Department of Defence
DSTO	Defence Science and Technology Organisation
FWHM	Full Width Half Maximum
HIL	Hardware In the Loop
IR	InfraRed
LOS	Line Of Sight
mat	MOSART atmospheric tool
MOSART	MOderate Spectral Atmospheric Radiance and Transmittance
MS	Missile Simulation
SGI	Silicon Graphics Incorporated
TERTEM	TERrain TEMperatures
texel	texture pixel
tmm	texture material mapper
US	United States
WSD	Weapons Systems Division
Zbits	Z-buffer **bits**

1. Introduction

SensorVision is a commercial-off-the-shelf (COTS) software package used in conjunction with Vega, a 3-D database visualisation software package developed by Paradigm Incorporated, to generate real-time infrared (IR) scenes[1]. SensorVision and Vega are built upon IRIS Performer and OpenGL on a Silicon Graphics machine with RealityEngine or InfiniteReality graphics capability. The Missile Simulation (MS) group in Weapons Systems Division (WSD) intends to use the SensorVision package to generate infrared (IR) scenes for hardware in the loop (HIL) missile simulations. This report discusses the radiometric equations implemented in SensorVision and identifies possible sources of errors resulting from approximations employed to achieve real-time performance. The level of error expected from the approximations, the validity of the SensorVision assumptions and the scenarios under which SensorVision may produce insufficiently accurate results are not discussed in this report. These topics will be treated in a subsequent report on the verification and validation of SensorVision.

SensorVision consists of a core library (sv) and two database construction tools referred to as the texture material mapper (tmm) and the MOSART atmospheric tool (mat).

- The core library (sv) performs the IR radiometric calculations and provides Vega with the required functionality to render IR scenes in real time. In addition, the sv library comprises a set of API (application programming interface) functions to define the sensor class and enable the user to set the sensor properties.
- The tmm tool is used to assign material properties to pixels on photographic textures and to produce the databases of material codes required by SensorVision.
- The mat generates run time databases for atmospheric quantities and for surface temperatures of scene materials. The mat comprises MOSART (moderate spectral atmospheric radiance and transmittance) and TERTEM (terrain temperatures)[2]. MOSART uses US DoD (United States Department of Defence) standard atmospheric codes to calculate the amount of radiation that reaches a unit area of earth for a particular geographical location, time period, weather condition and atmospheric profile. TERTEM estimates the temperature of a surface based on the level of incident radiation and the properties of the materials comprising that surface. The thermal history of the materials is not considered in the computations. TERTEM uses a one-dimensional three-layer model (surface and two layers) that includes four heat transfer fluxes: radiation, convection, conduction and evaporation. Mat is the main computational tool used in the evaluation of the SensorVision radiometric equations.

---

[1] SensorVision, in conjunction with Vega, is capable of image visualisation in any spectral band in the visible to the far infrared spectrums. Only the application of SensorVision to the generation of IR scenes will be considered in this report.

[2] MOSART and TERTEM were developed by Phillips Laboratory, Department of Geophysics, Air Force Material Command, Handscom AFB, MA 01731-3010.

It should be noted that various discrepancies exist between the information contained within this report and the formal documentation provided with SensorVision. Unfortunately, the SensorVision documentation was found to be inadequate, lacking in information and erroneous in some parts. Consequently, there are aspects of the SensorVision algorithm that are open to interpretation. To the authors' best knowledge and judgement, the information that is disclosed within this report is correct.

2. The SensorVision Radiometric Equations

SensorVision implements a radiometric equation for each pixel in the scene as part of the image visualisation process. The radiometric equation comprises only the following radiance quantities:

- $L_{solar/lunar}$ represents the in-band radiance detected by a sensor due to solar and/or lunar irradiation reflected specularly and diffusely from an object surface into the sensor.
- $L_{skyshine}$ represents the in-band radiance detected by a sensor due to emissions from the sky that are reflected from an object surface into the sensor.
- $L_{thermal}$ represents the in-band radiance detected by a sensor due to object surface emissions.
- L_{SVpath} represents the in-band radiance detected by a sensor due to atmospheric emissions and forward scattering along the path from the object surface to the sensor.

It should be noted that SensorVision has the capability to include the spectral response of the sensor in the radiance computations but it cannot model other sensor effects such as optical blur, noise and detector sampling. The radiometric equation [1][2] is given by (1) where each radiometric term is calculated by applying (2a), (2b), (2c) and (2d).

$$L_{observer} = L_{solar/lunar} + L_{skyshine} + L_{thermal} + L_{path} \qquad \left(Wcm^{-2}sr^{-1}\right) \quad (1)$$

$$L_{solar/lunar} = L^{*}_{direct}\cos\theta_i\rho\left(1-f_s\right)\tau_r + L^{*}_{direct}f_{sl}\left(\theta_r,\phi_r\right)\rho f_s N_s \tau_r \qquad \left(Wcm^{-2}sr^{-1}\right) \quad (2a)$$

$$L_{skyshine} = L^{*}_{ambient}\rho\tau_r \qquad \left(Wcm^{-2}sr^{-1}\right) \quad (2b)$$

$$L_{thermal} = L_{bb}\left(1-\rho\right)\tau_r \qquad \left(Wcm^{-2}sr^{-1}\right) \quad (2c)$$

$$L_{SVpath} = \frac{L^{*}_{path}}{1-\tau^{*}_{r}}\left(1-\tau_r\right) \qquad \left(Wcm^{-2}sr^{-1}\right) \quad (2d)$$

The parameter definitions are given below:

L_{direct} - Solar/lunar radiance incident on the object surface.
$L_{ambient}$ - Skyshine radiance incident on the object surface.
L_{bb} - Blackbody radiance emitted from the object surface.

L_{path} - Atmospheric path radiance for the line of sight path between the object surface and the sensor.

ρ - Diffuse reflection coefficient of the object surface.

τ_r - Atmospheric transmission coefficient for the line of sight path between the object surface and the sensor.

(θ_i, ϕ_i) - Angle of radiation incident on the object surface relative to the surface normal.

(θ_r, ϕ_r) - Angle of radiation reflected from the object surface relative to the surface normal.

f_s - Fraction of incident radiance reflected specularly.

$f_{sl}(\theta_r, \phi_r)$ - Angular dependence of the specularly reflected radiation.

N_s - Specular normalisation factor.

* - Indicates that the parameter is associated with only the centre pixel in the image frame.

Figure 1 shows a visual representation of the various radiance components considered in SensorVision.

In the following sections, each radiometric quantity in (1) is explained in detail and the appropriate radiance equation is derived. The SensorVision implementation of the equations is then described with emphasis on the approximations employed. SensorVision utilises various techniques to enable the real-time computation of the radiance terms [3]:

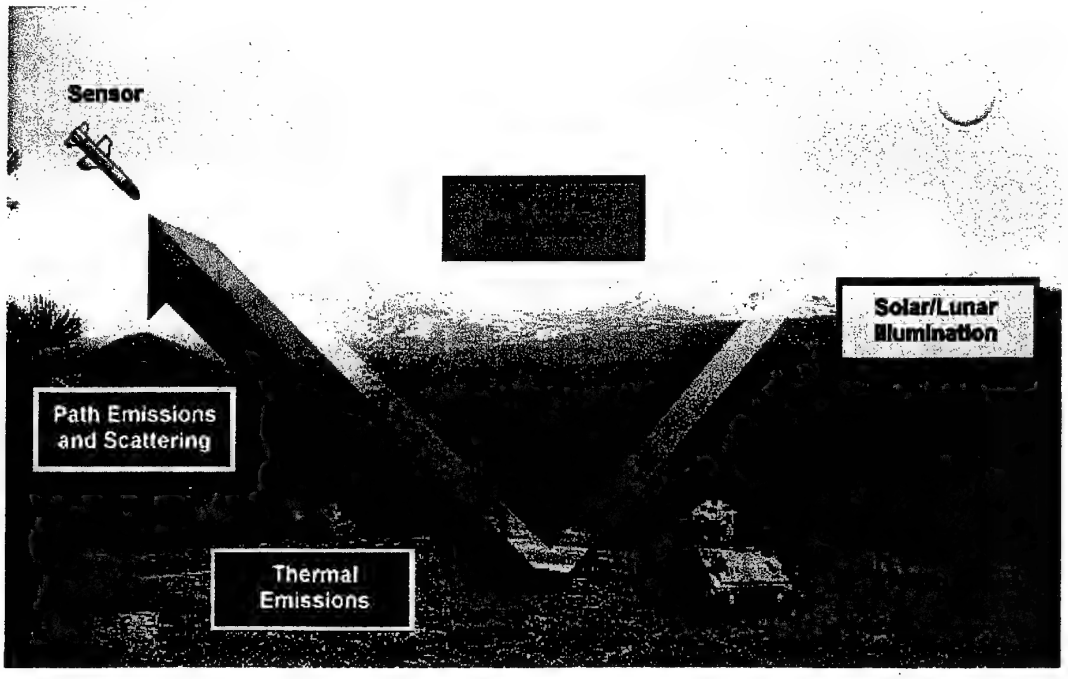

Figure 1: Diagram showing the radiance quantities considered in SensorVision.

- The main technique adopted involves the generation of various required quantities prior to the real-time simulation. The mat is used to create a multivariate database of the particular quantity of interest as a function of user defined variables. During run time, the quantity employed in the simulation is based on the instantaneous variable values and linear interpolation on the multivariate database. In order for this strategy to be implemented, the radiance equations need to be manipulated into forms that are compatible with the construction of the database. The resultant radiance equations, however, are not necessarily physically correct.
- Another approximation involves the physically accurate[3] calculation of only the radiance incident on the centre pixel in the image frame. The radiance impinging on off-centre pixels are computed by extrapolating the results of the central pixel case.
- In the integration of spectral radiance quantities over wavelength, SensorVision moves various spectral parameters outside the integral. Although not mathematically correct, this approximation is employed to force the equations to conform to the structure required for the generation of multivariate databases, and to allow the materials and atmospheric databases to be developed and maintained independently of each other.

The method in which the above approximations are employed will be clarified in the following discussions.

2.1 Thermal Emissions

2.1.1 Accurate Determination of Radiance Quantity

The radiometric equation yielding the radiance received by a sensor due to thermal emissions from a surface is derived from Planck's blackbody equation. The spectral radiance (L_λ^{bb}) emitted from a blackbody of temperature T is given by (3) where c_1 and c_2 are radiation constants given by (4a) and (4b), respectively. The subscript 'λ' is used to indicate the wavelength dependence of the blackbody spectral radiance.

$$L_\lambda^{bb} = \frac{c_1}{\pi\lambda^5\left(e^{c_2/\lambda T} - 1\right)} \qquad \left(Wm^{-2}sr^{-1}\mu m^{-1}\right) \tag{3}$$

$$c_1 = 3.7418 \times 10^8 \qquad \left(Wm^{-2}\mu m^4\right) \tag{4a}$$

$$c_2 = 1.438769 \times 10^4 \qquad \left(\mu mK\right) \tag{4b}$$

[3] Physically accurate in this sense means that the calculation of the radiance is accurate within the limitations of the MOSART atmospheric propagation code, which currently is an accepted standard for radiometric transfer calculations.

The integration of Planck's equation over all wavelengths of interest yields the radiance emitted from a blackbody within that waveband. Considering the normalised spectral response (φ_λ) of the particular sensor of interest, the spectral emissivity of the body[4] ($1-\rho_\lambda$) and the spectral atmospheric transmission ($\tau_{r\lambda}$) along the line of sight (LOS) path between the body and the sensor, the radiance detected by the sensor is given by (5).

$$L_{thermal} = \int_{\lambda_1}^{\lambda_2} \varphi_\lambda L_\lambda^{bb}(1-\rho_\lambda)\tau_{r\lambda} d\lambda \qquad \left(Wm^{-2}sr^{-1}\right) \qquad (5)$$

Given a particular scene model[5], the radiance due to thermal emissions is dependent only on the temperature of the body and the atmospheric transmission for the line of sight (LOS) path between the particular surface point and the detector. The temperature of the body, however, is calculated using MOSART and TERTEM based on the heating effects of the sun and the surrounding atmosphere. Consequently, the location of the sun and the profile of the surrounding atmosphere are required to calculate the radiance given by (5)

2.1.2 SensorVision Implementation

SensorVision implements an equation with a form that differs slightly from (5). The spectral emissivity and the atmospheric transmission coefficient are moved outside of the spectral integral. The resultant equations are therefore given by (6) and (7).

$$L_{thermal} = L_{bb}(1-\rho)\tau_r \qquad \left(Wcm^{-2}sr^{-1}\right) \qquad (6)$$

$$L_{bb} = \int_{\lambda_1}^{\lambda_2} \varphi_\lambda L_\lambda^{bb} d\lambda \qquad \left(Wcm^{-2}sr^{-1}\right) \qquad (7)$$

Mathematically, the spectral terms cannot be moved outside of the integral and this approximation generates errors in the result. The approximation, however, is reasonable if ρ_λ and $\tau_{r\lambda}$ are nearly constant in the spectral band of interest. The parameter values used in the calculation is the average reflection coefficient (ρ) and the average atmospheric transmission (τ_r) in the spectral band. Since only the average reflection coefficient is used in the calculation, all objects are essentially modelled as grey bodies.

---

[4] All materials are assumed to be opaque and Lambertian (diffuse) hence the spectral emissivity is simply ($1 - \rho_\lambda$).

[5] A complete scene model would include all material information on the objects in the scene as well as the sensor characteristics. The reflection coefficient ρ_λ, the spectral response of the sensor φ_λ and the spectral band ($\lambda_1 - \lambda_2$) are all defined.

It is anticipated that the above approximation will be reasonable in the 8 to 12 μm band but will likely generate errors in the 3 to 5 μm band. The rationale behind this statement is twofold. Firstly, the reflectance of materials tend to be invariant in the longer wavelength bands compared to the shorter wavelength bands. Secondly, the atmospheric transmission coefficient fluctuates significantly in the 3 to 5 μm band. High atmospheric attenuation occurs near 4.2 μm due to carbon dioxide absorption.

Each multiplicative term in (6) is computed separately in the manner described below.

Determination of Parameter L_{bb}

The calculation of the blackbody radiance (7), as seen by a specific detector, is dependent only on the temperature of the body. The surface temperatures are calculated prior to the real-time simulation by the mat. In the execution of the mat program, an input file is required in which the user sets the values of the variables affecting the temperature calculation. The atmospheric profile and the material list are defined along with the range of possible positions and orientations of surfaces. The expanse of time is also specified in the mat input file. Mat generates an output file that contains the temperature data for each user-defined:

- material;
- surface altitude;
- surface orientation azimuth;
- surface orientation slope; and
- the time of day.

The material data required in the temperature calculations performed by TERTEM is found in the directory[6] /usr/local/PSI/sv/materials/ht.

The five dimensional multivariate database computed by mat is stored in the file s*xx*.htt where *xx* is the atmospheric state number. During run time, in each image frame, SensorVision assigns a temperature to the vertices of all polygons in the 3-D scene. These temperatures are determined based on the location of each vertex, the orientation of the corresponding face normal and the current time. The material assigned to each vertex is either the material associated with the centre texel (texture pixel) or the texel closest to the polygon vertex. The choice is user selected. Texture-material associations are performed using the tmm tool. Having determined all required variables for an image frame, the vertex temperatures are extracted from the multivariate temperature database using linear interpolation on the five variables. The blackbody radiance is then computed for these vertex temperatures. The radiance emitted from any point on a polygon surface is calculated using trilinear interpolation on the radiance assigned to the vertices. The accuracy of the above procedure is dependent on the validity of the texture-material associations. Textures with shadows and multiple colour-material associations may generate misclassification errors. In

[6] The material database directory is designated by the MATERIALS_DATABASE system environment variable.

general, a polygon texture should only have one material association for accurate simulations. In addition, because a vertex is considered as a polygon attribute rather than an object attribute, it is possible to have more than one temperature assigned to the same object apex. This condition is unrealistic in real world environments.

The temperature data generated by TERTEM is not applicable to operated entities such as tanks or planes. Such objects should have temperatures manually assigned to the polygons [2].

The above discussion suggests that L_{bb} is calculated on a vertex basis since L_{bb} is computed accurately only at the vertices in the scene. The value of L_{bb} is approximated using interpolation for all other pixels in the image frame.

Determination of Parameter ρ

The reflection coefficient (ρ) for each pixel is calculated using the tmm generated files comprising the texture-material associations. The tmm output files are placed in the directory <texture_map_name>.tmm. Given the material composition of each texel, the reflection coefficient of the surface point corresponding to each pixel in the image frame can be computed based on the reflection coefficient data files in directory /usr/local/PSI/sv/materials/ref. As previously stated, the reflection coefficient value is the average spectral reflection coefficient over the waveband of interest.

The reflection coefficient is calculated on a pixel basis and the procedure described above is performed for all pixels in the scene.

Determination of Parameter τ_r

The atmospheric transmission coefficient for the LOS path between a surface point and the sensor is calculated by mat prior to the simulation. A multivariate database is generated for user-defined values of:

- the LOS range between the observer and the surface;
- the observer altitude; and
- the LOS elevation angle.

This database is stored in file s*xx*b*yy*.atmq for simulations of daytime and sxxbyy.lunar_atmq for simulations of nighttime. Variable *xx* and *yy* refer to the atmospheric state number and the spectral band number, respectively. The actual quantity calculated is given by (8), where r is the LOS range between the surface point and the sensor, and ln is the natural logarithm function.

$$\beta^* = \frac{-5.5r^*}{\ln(\tau_r^*)} \tag{8}$$

The superscript '*' identifies the quantities associated with the centre pixel in the image frame. During run time, SensorVision determines the LOS range, observer altitude and LOS elevation angle associated with only the centre pixel in the image frame. The parameter β^* for this LOS path is then extracted from the multivariate database using linear interpolation on the variables. The same β^* value is then assigned to all pixels in the image frame and the atmospheric transmission coefficient is calculated using (9) where r is the LOS range associated with each pixel.

$$\tau_r = e^{-5.5r/\beta^*} \tag{9}$$

This strategy essentially applies an exponential extrapolation on the atmospheric transmission coefficient based on the difference between the LOS range associated with a particular pixel and the LOS range at the centre pixel. The types of scene geometry in which this approximation is invalid will be discussed in a subsequent report on the verification and validation of SensorVision.

The atmospheric transmission coefficient is calculated on a scene by scene basis. This means that the transmission coefficient is calculated accurately for only one pixel in each frame. Approximations are then employed to determine the transmission coefficients for all other pixels in the frame.

Sources of Error

In summary, the following factors introduce errors in the SensorVision computation of the radiance due to object surface thermal emissions:

- Errors are introduced if the spectral reflection coefficient of materials in the IR scene vary significantly over the spectral band of interest.
- Errors occur if the spectral atmospheric transmission coefficient of the LOS path between the surface and the sensor fluctuates over the spectral band of interest.
- The thermal emission radiance computation has errors associated with the linear interpolation of the multivariate databases for temperature and the β^* parameter.
- Errors are introduced in the calculation of the emitted radiance from each point on an object face due to the interpolation of the face vertex radiance.
- There are errors associated with the exponential extrapolation of the atmospheric transmission coefficient.
- Poor choice of texture images in the scene modelling may generate texture-material misclassifications and contribute to errors in the SensorVision simulation.
- Materials that are not opaque or are non-Lambertian will be incorrectly modelled in SensorVision.

2.2 Path Emissions and Scattering

2.2.1 Accurate Determination of Radiance Quantity

Path emissions and forward scattering of radiation into the sensor are computed using the models employed in MOSART. The spectral path radiance from the surface to the sensor ($L_{path\,\lambda}$) is computed by MOSART and (10) is used to calculate the radiance detected by the sensor over the spectral band of interest. Parameter φ_λ is the normalised spectral response of the sensor.

$$L_{path} = \int_{\lambda_1}^{\lambda_2} \varphi_\lambda L_{path\,\lambda}\, d\lambda \qquad \left(Wm^{-2}sr^{-1}\right) \tag{10}$$

Given a particular scene model, the radiance due to path emissions and forward scattering in the LOS path between the surface and the sensor is dependent only on $L_{path\,\lambda}$, which in turn is dependent on the atmospheric profile between the surface and the sensor.

2.2.2 SensorVision Implementation

SensorVision essentially implements (10) with only one slight modification. Equation (10) is only accurately determined by the mat for the LOS path (between the surface and the sensor) corresponding to the centre pixel in the image frame. Consequently, (10) is implemented in the form of (11) where the superscript '*' refers to quantities associated with the LOS path at the centre pixel.

$$L_{SVpath} = \frac{L^*_{path}}{1-\tau_r^*}\left(1-\tau_r\right) \qquad \left(Wcm^{-2}sr^{-1}\right) \tag{11}$$

The path radiance associated with off-centre pixels is calculated using an extrapolation based on the fraction given by (12).

$$\frac{1-\tau_r}{1-\tau_r^*} \tag{12}$$

This fraction has an exponential dependency on the difference between the LOS range at the centre pixel compared to the LOS range at the off-centre pixel. The exponential dependency originates from the exponential form (9) of the transmission coefficient.

Determination of Parameter $L^*_{path}/(1-\tau^*_r)$

The mat performs the main component of the path radiance calculations prior to the simulation. The mat computes the quantity $L^*_{path}/(1-\tau^*_r)$ for each user-defined value of:

- the LOS range between the observer and the surface;
- the observer altitude;
- the LOS elevation angle;
- the direct source (sun or moon) elevation angle; and
- the direct source azimuth angle relative to the observer azimuth angle.

The results are stored in a multivariate database recorded in files s*xx*b*yy*.atmq for simulations of daytime and sxxbyy.lunar_atmq for simulations of nighttime. Variables *xx* and *yy* indicate the atmospheric state number and the spectral band number, respectively.

During run time, SensorVision determines the five parameters listed above associated with the centre pixel in each image frame. The parameter $L^*_{path}/(1-\tau^*_r)$ is then approximated using linear interpolation on the multivariate database. This same value is used in the radiance calculation of all pixels in the image frame.

Parameter $L^*_{path}/(1-\tau^*_r)$ is evaluated only once in each frame.

Determination of Parameter τ_r

The LOS ranges associated with all pixels are computed and the corresponding atmospheric transmission coefficient is determined using the strategy described in Section 2.1.2.

Sources of Error

In summary, the following factors introduce errors in the SensorVision computation of the path radiance quantity:

- There are errors associated with the linear interpolation of the multivariate databases for the $L^*_{path}/(1-\tau^*_r)$ quantity and the β^* parameter.
- Errors are associated with the exponential extrapolation of the atmospheric transmission coefficient.
- Errors are introduced because the path radiance at any pixel is assumed to be an exponential extrapolation on the value at the centre pixel.

2.3 Skyshine Reflections

2.3.1 Accurate Determination of Radiance Quantity

The radiometric equation giving the radiance detected by a sensor due to skyshine reflections is derived from the definition of hemispherical reflectance. By definition, the hemispherical spectral reflectance ($\rho_{h\lambda}$) is the ratio of the total spectral exitance over the reflected hemisphere to the total spectral irradiance over the incident hemisphere. Mathematically, the hemispherical spectral reflectance is given by (13).

$$\rho_{h\lambda} = \frac{\int_0^{2\pi}\int_0^{\pi/2} L_{r\lambda}(\theta_r,\phi_r)\cos\theta_r \sin\theta_r d\theta_r d\phi_r}{\int_0^{2\pi}\int_0^{\pi/2} L_{i\lambda}(\theta_i,\phi_i)\cos\theta_i \sin\theta_i d\theta_i d\phi_i} \tag{13}$$

The parameter L is the radiance while (θ,ϕ) is the angle of the incident or reflected radiation relative to the surface normal. All variables with subscript 'r' are reflected quantities while those with subscript 'i' are incident quantities. The integration of the projected solid angle is over the entire upper hemisphere. Assuming the reflecting surface is Lambertian (ie. $L_{r\lambda}$ is independent of θ_r and ϕ_r) the diffuse spectral reflectance (ρ_λ) is given by (14).

$$\rho_\lambda = \frac{L_{r\lambda}\int_0^{2\pi}\int_0^{\pi/2} \cos\theta_r \sin\theta_r d\theta_r d\phi_r}{\int_0^{2\pi}\int_0^{\pi/2} L_{i\lambda}(\theta_i,\phi_i)\cos\theta_i \sin\theta_i d\theta_i d\phi_i} \tag{14}$$

The integration over the reflected hemisphere in the numerator is π, hence (14) can be simplified to give (15).

$$\rho_\lambda = \frac{L_{r\lambda}\pi}{\int_0^{2\pi}\int_0^{\pi/2} L_{i\lambda}(\theta_i,\phi_i)\cos\theta_i \sin\theta_i d\theta_i d\phi_i} \tag{15}$$

Rearranging (15) so that the reflected spectral radiance is the subject of the equation results in (16).

$$L_{r\lambda} = \frac{\rho_\lambda}{\pi}\int_0^{2\pi}\int_0^{\pi/2} L_{i\lambda}(\theta_i,\phi_i)\cos\theta_i \sin\theta_i d\theta_i d\phi_i \qquad \left(Wm^{-2}sr^{-1}\mu m^{-1}\right) \tag{16}$$

Considering the atmospheric attenuation due to the line of sight transmission from the surface to the observer ($\tau_{r\lambda}$), the spectral radiance incident on the sensor is given by (17).

$$L_{skyshine\lambda} = \frac{\rho_\lambda \tau_{r\lambda}}{\pi} \int_0^{2\pi} \int_0^{\pi/2} L_{i\lambda}(\theta_i, \phi_i) \cos\theta_i \sin\theta_i d\theta_i d\phi_i \qquad \left(Wm^{-2} sr^{-1} \mu m^{-1}\right) \tag{17}$$

The radiance detected by the sensor due to skyshine reflections is therefore given by (18), taking into account the spectral response of the sensor.

$$L_{skyshine} = \int_{\lambda_1}^{\lambda_2} \frac{\varphi_\lambda \rho_\lambda \tau_{r\lambda}}{\pi} \int_0^{2\pi} \int_0^{\pi/2} L_{i\lambda}(\theta_i, \phi_i) \cos\theta_i \sin\theta_i d\theta_i d\phi_i d\lambda \qquad \left(Wm^{-2} sr^{-1}\right) \tag{18}$$

The spectral radiance quantity ($L_{i\lambda}$) is dependent on the angles (θ_i, ϕ_i) and is the ambient radiant emissions from the atmosphere. It is calculated using the MOSART atmospheric tool. The surface point location, the sensor location, the position of the sun/moon and the atmospheric profile are all required to evaluate (18).

2.3.2 SensorVision Implementation

The SensorVision computation of the radiance due to skyshine reflections is based on (19) and (20).

$$L_{skyshine} = L^*_{ambient} \rho \tau_r \qquad \left(Wcm^{-2} sr^{-1}\right) \tag{19}$$

$$L^*_{ambient} = \frac{\int_{\lambda_1}^{\lambda_2} \frac{\varphi_\lambda \tau^*_{r\lambda}}{\pi} \int_0^{2\pi} \int_0^{\pi/2} L_{i\lambda}(\theta_i, \phi_i) \cos\theta_i \sin\theta_i d\theta_i d\phi_i d\lambda}{\tau^*_r} \qquad \left(Wcm^{-2} sr^{-1}\right) \tag{20}$$

This equation form has been adopted because the radiance associated with skyshine reflections is calculated accurately only for the centre pixel in each image frame. The radiance at off-centre image pixels are approximated and assumed to be related to the radiance at the centre pixel by the ratio τ_r / τ^*_r. This technique essentially uses an exponential function to extrapolate the radiance incident on off-centre pixels given the radiance at the centre pixel.

Compared to (18), the SensorVision implementation based on (19) and (20) moves the reflection coefficient term outside of the spectral integration.

Determination of Parameter $L^*_{ambient}$

The mat accurately computes the value of $L^*_{ambient}$ for user-defined values of:

- the LOS range between the observer and the surface;
- the observer altitude;
- the LOS elevation angle; and
- the direct source (sun or moon) elevation angle.

The results form a multivariate database that is stored in files s*xx*b*yy*.atmq and sxxbyy.lunar_atmq.

During run time, SensorVision determines the value of $L^*_{ambient}$ for the centre pixel using linear interpolation on the multivariate database. This quantity is calculated only once for each frame and is assumed to be the same for all pixels in the image frame.

Determination of Parameters ρ and τ_r

The reflection coefficient and the transmission coefficient for all pixels in the image frame are computed using the strategies described in Section 2.1.2.

Sources of Error

The following factors introduce errors in the SensorVision computation of the radiance due to skyshine reflections:

- There are errors associated with the linear interpolation of the multivariate databases for the $L^*_{ambient}$ quantity and the β^* parameter.
- Errors are generated due to the exponential extrapolation of the atmospheric transmission coefficient parameter.
- Errors are introduced because the radiance due to skyshine reflections at any pixel is assumed to be an exponential extrapolation on the value at the centre pixel.
- Errors occur if the reflection coefficient of materials in the IR scene varies significantly over the band of interest.
- Materials that are non-Lambertian are incorrectly treated by SensorVision.

2.4 Solar/Lunar Reflections

The equation giving the radiance due to solar/lunar reflections can be separated into two components comprising the diffuse and specular terms, as given by (21).

$$L_{solar/lunar} = L_{\substack{solar/lunar \\ specular}} + L_{\substack{solar/lunar \\ diffuse}} \tag{21}$$

2.4.1 Solar/Lunar Diffuse Reflections

The diffuse component of radiance due to reflections resulting from solar or lunar radiation is derived from the definition of the diffuse spectral reflectance. The diffuse spectral reflectance is defined as the ratio of the reflected spectral exitance to the incident spectral irradiance. Since the incident spectral radiance originating from the sun or moon is constant, the spectral irradiance is given by the product of the spectral

radiance ($L_{i\lambda}$) and the projected solid angle ($\Omega\cos\theta_i$) of the sun or the moon. Consequently, the diffuse spectral reflectance of a surface is given by (22), where π is the projected solid angle over the reflected hemisphere.

$$\rho_\lambda = \frac{L_{r\lambda}\pi}{L_{i\lambda}\Omega\cos\theta_i} \tag{22}$$

Rearranging (22) so that the reflected radiance is the focus of the equation results in (23).

$$L_{r\lambda} = \frac{\rho_\lambda}{\pi} L_{i\lambda}\Omega\cos\theta_i \qquad \left(Wm^{-2}sr^{-1}\mu m^{-1}\right) \tag{23}$$

Replacing the incident spectral radiance ($L_{i\lambda}$) by the spectral radiance of the sun or the moon ($L_{sun/moon\,\lambda}$) and substituting in the formula for the solid angle yields (24).

$$L_{r\lambda} = \frac{\rho_\lambda}{\pi} L_{sun/moon\,\lambda} \frac{A_{sun/moon}}{R_i^2}\cos\theta_i \qquad \left(Wm^{-2}sr^{-1}\mu m^{-1}\right) \tag{24}$$

The parameter $A_{sun/moon}$ is the projected area of the solar or lunar disk and R_i is the distance between the reflecting surface and that disk. Only a proportion of the incident radiance is reflected diffusely hence a multiplicative fractional term $\left(1-f_{s\lambda}\right)$ is incorporated into the right hand side of (24). The parameter $f_{s\lambda}$ is the proportion of the incident spectral irradiance that is reflected specularly. In addition, the atmospheric attenuation due to the incident LOS path and the reflected LOS path should be included in the equation. The resultant equation is therefore given by (25).

$$L_{r\lambda} = \frac{\rho_\lambda}{\pi}\tau_{r\lambda} L_{sun/moon\,\lambda} \frac{A_{sun/moon}}{R_i^2}\tau_{i\lambda}\cos\theta_i\left(1-f_{s\lambda}\right) \qquad \left(Wm^{-2}sr^{-1}\mu m^{-1}\right) \tag{25}$$

Integrating (25) over the frequency band of interest and incorporating the spectral response of the sensor results in (26).

$$L_{\substack{solar/lunar\\diffuse}} = \frac{A_{sun/moon}}{\pi R_i^2}\cos\theta_i \int_{\lambda_1}^{\lambda_2} \varphi_\lambda L_{sun/moon\,\lambda}\rho_\lambda\tau_{r\lambda}\tau_{i\lambda}\left(1-f_{s\lambda}\right)d\lambda \qquad \left(Wm^{-2}sr^{-1}\right) \tag{26}$$

It is clear that the surface point location, the detector location, the source location and the atmospheric profile are all required in the computation of (26).

2.4.2 Solar/Lunar Specular Reflections

The equation giving the radiance due to solar or lunar specular reflections has a form similar to that of (26). The spectral irradiance incident on the reflecting surface including the effects of atmospheric attenuation is given by (27).

$$E_{i\lambda} = L_{sun/moon\,\lambda} \frac{A_{sun/moon}}{R_i^2} \cos\theta_i \tau_{i\lambda} \qquad \left(Wm^{-2}\mu m^{-1}\right) \tag{27}$$

If the fraction $\rho_\lambda (1 - f_{s\lambda})$ of the spectral irradiance is reflected diffusely then the remaining proportion, given by $\rho_\lambda f_{s\lambda}$, must be reflected specularly. The total specularly reflected spectral exitance is therefore given by (28).

$$M_{r\lambda} = L_{r\lambda}\pi = L_{sun/moon\,\lambda} \frac{A_{sun/moon}}{R_i^2} \cos\theta_i \tau_{i\lambda} \rho_\lambda f_{s\lambda} \qquad \left(Wm^{-2}\mu m^{-1}\right) \tag{28}$$

The specularly reflected radiance for a particular sensor location in the reflected hemisphere is dependent on the properties of the specular lobe and the direction of the reflected ray that would satisfy Snell's law. Figure 2 illustrates the concept of the specular lobe.

The specular lobe effects can be modelled by introducing a parameter $f_{sl\lambda}(\theta_r, \phi_r)$ which represents the lobe amplitude in a particular direction in the reflected hemisphere. This parameter should have a maximum value of unity in the classical Snell's law direction and should decrease proportionally with the lobe size as the observer direction departs from the Snell's law direction. In addition, a normalising factor $N_{s\lambda}$ needs to be included in order to ensure that conservation of energy is satisfied. The energy associated with the specular emittance of (28) must be conserved

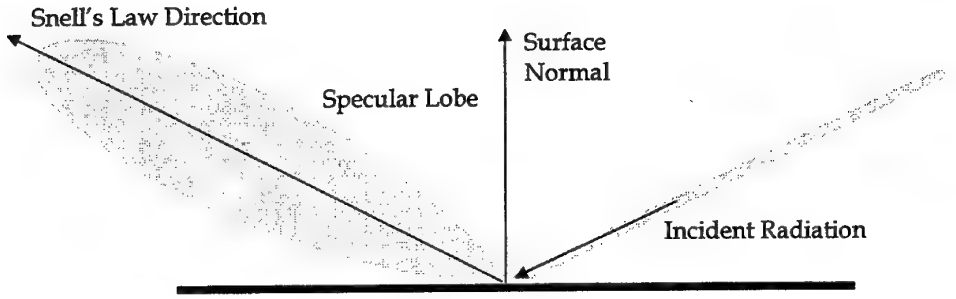

Figure 2: Diagram illustrating the concept of specular reflection.

when redirected in a manner conforming to the shape of the specular lobe. Consequently, the energy which was previously emitted diffusely over the entire upper hemisphere (2π) is now only emitted in the solid angle defined by the specular lobe. The conversation of energy equation is therefore given by (29) and the normalisation factor is defined by (30).

$$2\pi = N_{s\lambda} \int_0^{2\pi} \int_0^{\pi/2} f_{sl\lambda}(\theta_r, \phi_r) d\theta_r d\phi_r \tag{29}$$

$$N_{s\lambda} = \frac{2\pi}{\int_0^{2\pi} \int_0^{\pi/2} f_{sl\lambda}(\theta_r, \phi_r) d\theta_r d\phi_r} \tag{30}$$

The specularly reflected spectral exitance in a given direction is therefore given by (31).

$$M_{r\lambda}(\theta_r, \phi_r) = L_{r\lambda}(\theta_r, \phi_r)\pi = L_{sun/moon\,\lambda} \frac{A_{sun/moon}}{R_i^2} \cos\theta_i \tau_{i\lambda} \rho_\lambda f_{s\lambda} N_{s\lambda} f_{sl\lambda}(\theta_r, \phi_r) \quad \left(Wm^{-2}\mu m^{-1}\right) \tag{31}$$

Consequently, the spectral radiance incident on a detector, taking into account the atmospheric attenuation of the path from the surface to the observer, is given by (32).

$$L_{r\lambda}(\theta_r, \phi_r) = \frac{1}{\pi} L_{sun/moon\,\lambda} \frac{A_{sun/moon}}{R_i^2} \cos\theta_i \tau_{i\lambda} \rho_\lambda f_{s\lambda} N_{s\lambda} f_{sl\lambda}(\theta_r, \phi_r) \tau_{r\lambda} \quad \left(Wm^{-2}sr^{-1}\mu m^{-1}\right) \tag{32}$$

The radiance incident on a sensor due to solar or lunar specular reflections is given by (33).

$$L_{\substack{solar/lunar \\ specular}}(\theta_r, \phi_r) = \frac{A_{sun/moon}}{\pi R_i^2} \int_{\lambda_1}^{\lambda_2} \varphi_\lambda L_{sun/moon\,\lambda} \rho_\lambda \tau_{r\lambda} \tau_{i\lambda} f_{s\lambda} \cos\theta_i N_{s\lambda} f_{sl\lambda}(\theta_r, \phi_r) d\lambda \quad \left(Wm^{-2}sr^{-1}\right) \tag{33}$$

It is again apparent that the surface point location, the detector location, the source location and the atmospheric profile are all required in the determination of (33).

2.4.3 SensorVision Implementation

The radiance due to solar or lunar reflections is calculated in SensorVision using (34), (35) and (36).

$$L_{\substack{solar/lunar \\ diffuse}} = L^*_{direct} \cos\theta_i \rho\left(1 - f_s\right)\tau_r \qquad \left(Wcm^{-2}sr^{-1}\right) \qquad (34)$$

$$L_{\substack{solar/lunar \\ specular}} = L^*_{direct} f_{sl}\left(\theta_r, \phi_r\right)\rho f_s N_s \tau_r \qquad \left(Wcm^{-2}sr^{-1}\right) \qquad (35)$$

$$L^*_{direct} = \frac{A_{sun/moon}}{\pi R_i^2} \frac{\int_{\lambda_1}^{\lambda_2} \varphi_\lambda L_{sun/moon\,\lambda} \tau_{i\lambda} \tau^*_{r\lambda} d\lambda}{\tau^*_r} \qquad \left(Wcm^{-2}sr^{-1}\right) \qquad (36)$$

Compared to (26) and (33), the reflection coefficient and the specular parameters have been moved outside of the spectral integration. Consequently, these terms must be approximately constant in the spectral band of interest if errors are to be avoided. Most of the strategies employed in Section 2.3.2 are again adopted. The radiance due to solar/lunar specular or diffuse reflections at a pixel in the image frame is assumed to be related to that at the centre pixel by the fraction τ_r / τ^*_r. This essentially represents an exponential extrapolation on the centre pixel radiance based on the difference between the LOS range associated with a particular pixel compared to the LOS range at the centre pixel.

Determination of Parameter L^*_{direct}

The quantity L^*_{direct} is computed by mat for user-defined values of:

- the LOS range between the observer and the surface;
- the observer altitude;
- the LOS elevation angle; and
- the sun or moon elevation angle.

The resultant multivariate database is stored in files s*xx*b*yy*.atmq and sxxbyy.lunar_atmq.

During run time, SensorVision determines the value of L^*_{direct} for the centre pixel in each image frame. This quantity is calculated only once for each frame and is used in the radiance calculation for all pixels in the image frame.

Determination of Parameters ρ and τ_r

Parameters ρ and τ_r are computed for all pixels in the image frame using the methodologies described in Section 2.1.2.

Determination of Parameters f_s, $f_{sl}(\theta_r, \phi_r)$ and N_s

The specular characteristics of the surface, namely the fraction of radiance reflected specularly and the specular lobe bandwidth, are defined in the material definitions. The function $f_{sl}(\theta_r, \phi_r)$ is dependent on the unit vectors illustrated in Figure 3. Vector $\hat{n}$ is the surface normal, $\hat{i}$ is the direction unit vector from the surface to the sun or moon and $\hat{r}$ is the direction unit vector from the surface to the observer. The unit vector $\hat{s}$ is defined as the normalised vector summation of $\hat{i}$ and $\hat{r}$, and is given by (37).

$$\hat{s} = \frac{\hat{i} + \hat{r}}{\left\| \hat{i} + \hat{r} \right\|} \tag{37}$$

The specular lobe function is defined by (38) where χ is the dot product of $\hat{s}$ and $\hat{n}$, and the shininess parameter defines the angular bandwidth of the specular lobe.

$$f_{sl}(\theta_r, \phi_r) = \chi^{shininess} \tag{38}$$

$$\chi = \hat{s} \bullet \hat{n} \tag{39}$$

Physically, χ is the cosine of the angle between the surface normal vector and the unit vector $\hat{s}$. The angle between $\hat{n}$ and $\hat{s}$ is labelled γ in Figure 3. Since the specular lobe function is defined relative to the Snell's law direction, the relationship between α and γ need to be established, where α is the angle between $\hat{r}$ and the Snell's law direction. Geometrical analysis of the vector diagram shown in Figure 3 reveals that the relationship between the pertinent angles is given by (40).

$$\alpha = 2\gamma \tag{40}$$

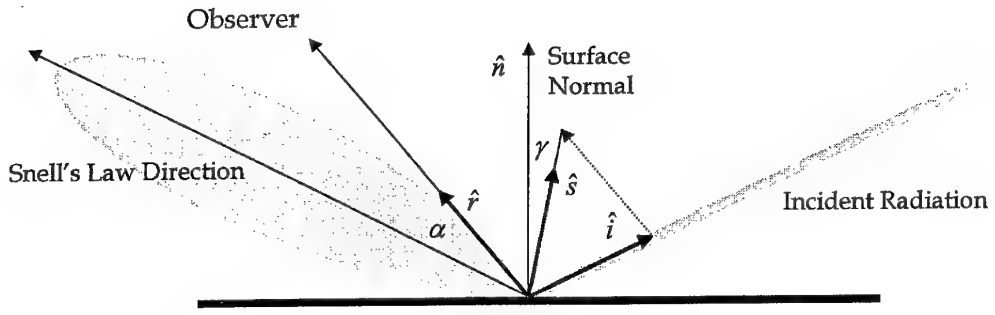

Figure 3: Diagram showing unit vectors associated with definition of specular lobe function.

Consequently, (39) can be expressed in the form of (41).

$$\chi = \hat{s} \bullet \hat{n} = \cos\left(\frac{\alpha}{2}\right) \tag{41}$$

From the definitions given by (38) and (41), it is clear that $f_{sl}(\theta_r, \phi_r)$ has a value of one in the Snell's law direction and decreases as the observer direction departs from the Snell's law direction. The rate of decrease is dependent on the shininess parameter which sets the specular lobe angular bandwidth. The shininess parameter is defined by (42) and is derived from the fact that $f_{sl}(\theta_r, \phi_r)$ has a value of 0.5 when $\alpha = BW/2$ and $\chi = \cos(BW/4)$. The parameter BW is the full width half maximum (FWHM) bandwidth of the specular lobe.

$$shininess = \frac{\log 0.5}{\log\left(\cos\left(\frac{BW}{4}\right)\right)} \tag{42}$$

As described in Section 2.4.2, the specular normalisation factor is determined by applying the conservation of energy law. The only difference in the SensorVision implementation is that the $\cos\theta_i$ term in (33) is lumped into the specular normalisation definition. Consequently, no $\cos\theta_i$ term appears in (35). The equation for N_s is therefore defined by (43).

$$N_s = \frac{2\pi \cos\theta_i}{\int_0^{2\pi} \int_0^{\pi/2} f_{sl}(\theta_r, \phi_r) d\theta_r d\phi_r} \tag{43}$$

SensorVision uses a look up table to determine N_s given the shininess parameter. The N_s parameter was determined by calculating the correct specular normalisation factor for six different light source directions (0°, 15°, 30°, 45°, 60° and 75°) and averaging the results [1][2]. Table 1 shows the N_s values used by SensorVision for the various specular lobe bandwidths and the corresponding shininess parameters. The last two columns of Table 1 indicate the minimum and maximum errors between the average result and the six values calculated for the six different light source directions. This table shows that significant errors are associated with the N_s value for large specular lobe bandwidths. Note also that the specular lobe bandwidth must be greater than 24° due to current Silicon Graphics hardware limitations.

Material specular properties are defined in data files located in the directory /usr/local/PSI/sv/materials/spec. The file /usr/local/PSI/sv/materials/mat

specifies the specular data file associated with each material. The specular capabilities of the current version of SensorVision are still in development and the existing set of specular data files is meagre. Furthermore, the specular properties are set on a per texture basis. The specular properties are calculated once only for each texture in the image scene.

Sources of Error

In summary, the following factors introduce errors in the SensorVision computation of the radiance due to solar/lunar reflections:

- There are errors associated with the linear interpolation of the multivariate databases for the L^{*}_{direct} quantity and the β^{*} constant.
- Errors are generated due to the exponential extrapolation of the atmospheric transmission coefficient parameter.
- Errors are introduced because the radiance at any pixel is assumed to be an exponential extrapolation on the value at the centre pixel.
- Errors occur in the computation of the specular normalisation factor, especially if the specular lobe bandwidth is large.
- Errors occur if the reflection coefficient and the specular parameters of materials in the IR scene vary significantly over the band of interest.
- Materials that are not Lambertian are incorrectly modelled in SensorVision.

FWHM BW	Shininess Parameter	N_s	Minimum N_s error	Maximum N_s error
23.83	128.00	32.64	-0.43 %	+2.16 %
25	116.27	29.72	-0.51 %	+2.36 %
30	80.67	20.82	-0.73 %	+3.08 %
35	59.21	15.44	-0.89 %	+3.33 %
40	45.28	11.94	-1.01 %	+3.11 %
45	35073	9.54	-1.13 %	+2.46 %
50	28.89	7.81	-1.12 %	+2.17 %
55	23.84	6.54	-1.21 %	+2.75 %
60	19.99	5.57	-1.24 %	+3.29 %
65	17.00	4.81	-1.19 %	+3.70 %
70	14.63	4.22	-4.22 %	+3.89 %
75	12.71	3.73	-5.63 %	+4.18 %
80	11.14	3.34	-7.6 %	+4.0 %
85	9.84	3.02	-9.4 %	+3.9 %
90	8.75	2.75	-11 %	+4.2 %
180	2.00	1.13	-40 %	+18 %

Table 1: Shininess values and specular normalisation values for various specular lobe bandwidths.

3. Rendering Operations

There are several issues pertaining to the Vega rendering of the IR scene generated by SensorVision that needs to be addressed. These factors are predominantly limitations associated with Vega, Performer or the SGI (Silicon Graphics Incorporated) hardware[7] but their effects on SensorVision are important considerations in the determination of the overall simulation accuracy.

3.1 Pixel Bit Resolution

The radiance quantities calculated by SensorVision must be quantised into pixel values for storage in the frame buffer. The resolution of the quantisation process is dependent on the number of colour bits (cbits) set in the frame buffer and the full range of radiance values to be displayed. The number of cbits is optimised by the Silicon Graphics hardware and is dependent on other frame buffer requirements. The current limit in the SGI hardware is 12 cbits. The user can set the radiance range by defining the minimum and maximum temperatures in the scene. Specifying the temperature range is appropriate for emission-dominated scenes but it may be difficult to relate temperatures to absolute radiance in simulations with significant amounts of reflections [4]. The range of absolute radiance can be specified indirectly by manually setting the buffer parameters associated with the radiance to pixel value mapping equation. A radiance (L) is mapped to a pixel value (n) in the range 0 to $2^N - 1$ using (44), where N is the number of cbits.

$$n = \mathrm{int}\left(2^N BG\left(\frac{L}{G} - DC\right) - 0.5\right) \tag{44}$$

Parameter BG is the accumulation buffer gain, G is the gain control multiplier and DC is the accumulation buffer offset. Function int rounds the argument to the nearest integer. Note that the ratio L/G is limited to the range 0 to 1. If the buffer parameters are chosen poorly, significant errors can arise in the simulation due to saturation effects, base value limiting and poor resolution. Since the current version of SensorVision does not allow access to the computed scene radiance prior to the frame buffer mapping, the pixel bit resolution is a dominant consideration in the application of SensorVision for HIL simulations.

[7] The SGI hardware, referred to in this report, is an Onyx2 machine with an InfiniteReality2 graphics engine.

3.2 The Depth Buffer

The digitisation problem is also evident in the use of the depth buffer (or Z-buffer) to provide LOS range information to SensorVision. The LOS range is an important parameter in the calculation of radiometric quantities due to atmospheric path effects. The current SGI hardware limits the number of Z-buffer bits (Zbits) to 23. The resolution and limits of the range information is set by the near and far field clipping plane specifications. Unfortunately, documentation on the use of the Z-buffer in SensorVision is non-existent and it is currently not known how the range information is mapped into the Z-buffer. In symmetric frustrum projection, the mapping function appears to have a hyperbolic form.

3.3 Aliasing

Aliasing is a problem that occurs in the pixelisaton of a scene [5] whereby scene features are distorted or omitted due to the relative size of the feature compared to the pixel size. Vega performs anti-aliasing by passing multiple samples of the scene through each pixel. Such a technique is adequate for visual simulations but not for IR missile HIL testing. Reference [4] has shown that the total radiant intensity of a scene can vary as a function of pixel size, even when anti-aliasing has been employed. This result is inconsistent with real world expectations.

4. Conclusions

This report has provided a comprehensive description of the radiometric equations employed by SensorVision. The accurate radiance equations were derived and the SensorVision implementations of those equations were outlined. The emphasis in this report has been to highlight all possible sources of errors in the SensorVision computation and to elucidate the reasons why certain methodologies are employed. The sacrifice of accuracy for real-time performance means that SensorVision should be used with caution in certain HIL simulations. The main factors identified as being likely to generate errors in SensorVision simulations are as follows:

- Materials with spectral reflection coefficients that fluctuate over the spectral band of interest may cause significant quantitative errors in the radiance calculation. In addition, the use of the average atmospheric transmission coefficient rather than its spectral equivalent affects the accuracy of the calculation.
- The use of exponential extrapolation to approximate pixel radiance values based on the radiance incident on the centre pixel of an image may produce unacceptable errors in some IR scenes.
- Limitations of Vega and the SGI hardware (colour bit resolution, Z-buffer resolution and aliasing) may generate errors if certain simulation parameters are not optimised for the particular simulation of interest. For example, the gain and DC offset settings associated with the mapping of radiance to pixel values should be optimised to reduce pixel bit resolution errors.

There is a need to validate the SensorVision algorithm and quantify the expected error levels in a simulation. The MS group of WSD is currently undertaking this task and subsequent reports, which will document the results of the verification and validation process, are planned.

5. References

[1] SensorVision Online Documentation, *specular_norm.doc.*

[2] D. C. Anding, SensorVision Technical Description, Paradigm Simulation Incorporated, April 28, 1998.

[3] D. C. Anding and A. Szabo, *Real-Time Image Visualisation for Sensors.*

[4] *Independent Assessment of the Accuracy and Useability of SensorVision,* Wright Laboratory, Armament Directorate, Advance Guidance Division, Eglin, AFB, 27 May 1997.

[5] M. Woo, J. Neider and T. Davis, *OpenGL Programming Guide - Second Edition,* Addison-Wesley, 1997.

DISTRIBUTION LIST

SensorVision Radiometric Equations (Version 2.2)

Ninh Duong and Michael Wegener

AUSTRALIA

DEFENCE ORGANISATION

Task Sponsor
DASD
S&T Program
Chief Defence Scientist
FAS Science Policy
AS Science Corporate Management
} shared copy
Director General Science Policy Development
Counsellor Defence Science, London (Doc Data Sheet)
Counsellor Defence Science, Washington (Doc Data Sheet)
Scientific Adviser to MRDC Thailand (Doc Data Sheet)
Scientific Adviser Policy and Command
Navy Scientific Adviser (Doc Data Sheet and distribution list only)
Scientific Adviser - Army (Doc Data Sheet and distribution list only)
Air Force Scientific Adviser
Director Trials

Electronics and Surveillance Research Laboratory
Head Electro-Optical Counter Measures Group (EWD)
Head Signal Measurement and Analysis Group (EWD)
Head Image Analysis and Exploitation Group (SSD)
Head Signature Management (SSD)
Mr Geoff Burls (SSD)

Aeronautical and Maritime Research Laboratory
Director

Chief of Weapon Systems Division
Research Leader Maritime Weapons Systems (WSD)
Research Leader Air Weapons Systems (WSD)
Research Leader Land Weapons Systems (WSD)
Research Leader Joint and Intelligence (WSD)
Head Missile Simulation Group (WSD)
Head Electro-Optical Seekers (WSD)
Head Advance Concepts (WSD)
Head Weapons Systems Analysis (WSD)
Michael Wegener (WSD)
Ninh Duong (WSD)

DSTO Library and Archives
Library Fishermens Bend
Library Maribyrnong
Library Salisbury (2 copies)
Australian Archives
Library, MOD, Pyrmont (Doc Data sheet only)
*US Defense Technical Information Center, 2 copies
*UK Defence Research Information Centre, 2 copies
*Canada Defence Scientific Information Service, 1 copy
*NZ Defence Information Centre, 1 copy
National Library of Australia, 1 copy

Capability Development Division
Director General Maritime Development (Doc Data Sheet only)
Director General Land Development (Doc Data Sheet only)
Director General C3I Development (Doc Data Sheet only)
Director General Aerospace Development

Army
ABCA Office, G-1-34, Russell Offices, Canberra (4 copies)
SO (Science), DJFHQ(L), MILPO Enoggera, Queensland 4051 (Doc Data Sheet only)
NAPOC QWG Engineer NBCD c/- DENGRS-A, HQ Engineer Centre Liverpool Military Area, NSW 2174 (Doc Data Sheet only)

Intelligence Program
DGSTA Defence Intelligence Organisation

Corporate Support Program
OIC TRS, Defence Regional Library, Canberra

UNIVERSITIES AND COLLEGES
Australian Defence Force Academy
Library
Head of Aerospace and Mechanical Engineering
Senior Librarian, Hargrave Library, Monash University
Librarian, Flinders University

OTHER ORGANISATIONS
NASA (Canberra)
AGPS
DERA (Malvern)

OUTSIDE AUSTRALIA

ABSTRACTING AND INFORMATION ORGANISATIONS
Library, Chemical Abstracts Reference Service
Engineering Societies Library, US
Materials Information, Cambridge Scientific Abstracts, US
Documents Librarian, The Center for Research Libraries, US

INFORMATION EXCHANGE AGREEMENT PARTNERS

Acquisitions Unit, Science Reference and Information Service, UK
Library - Exchange Desk, National Institute of Standards and Technology, US
National Aerospace Laboratory, Japan
National Aerospace Laboratory, Netherlands

SPARES (5 copies)

Total number of copies: **63**

DEFENCE SCIENCE AND TECHNOLOGY ORGANISATION
DOCUMENT CONTROL DATA

1. PRIVACY MARKING/CAVEAT (OF DOCUMENT)

2. TITLE

SensorVision Radiometric Equations
Version 2.2

3. SECURITY CLASSIFICATION (FOR UNCLASSIFIED REPORTS THAT ARE LIMITED RELEASE USE (L) NEXT TO DOCUMENT CLASSIFICATION)

Document	(U)
Title	(U)
Abstract	(U)

4. AUTHOR(S)

Ninh Duong and Michael Wegener

5. CORPORATE AUTHOR

Aeronautical and Maritime Research Laboratory
PO Box 4331
Melbourne Vic 3001 Australia

6a. DSTO NUMBER	6b. AR NUMBER	6c. TYPE OF REPORT	7. DOCUMENT DATE
DSTO-TN-0193	AR-010-833	Technical Note	February 1999

8. FILE NUMBER	9. TASK NUMBER	10. TASK SPONSOR	11. NO. OF PAGES	12. NO. OF REFERENCES
J9505/15/164	AIR 96/194	DASD	23	5

13. DOWNGRADING/DELIMITING INSTRUCTIONS

14. RELEASE AUTHORITY

Chief, Weapons Systems Division

15. SECONDARY RELEASE STATEMENT OF THIS DOCUMENT

Approved for public release

OVERSEAS ENQUIRIES OUTSIDE STATED LIMITATIONS SHOULD BE REFERRED THROUGH DOCUMENT EXCHANGE CENTRE, DIS NETWORK OFFICE, DEPT OF DEFENCE, CAMPBELL PARK OFFICES, CANBERRA ACT 2600

16. DELIBERATE ANNOUNCEMENT

No Limitations

17. CASUAL ANNOUNCEMENT Yes

18. DEFTEST DESCRIPTORS

Infrared Images, Image Generation (Computers), Radiometry

19. ABSTRACT

This technical note describes the radiometric equations employed by an IR scene generation COTS software package called SensorVision. The components of the radiometric equations used to compute the radiance quantities of an IR scene are discussed in detail and assumptions used in the derivation of these equations are identified. The focus of this technical note is to highlight possible sources of errors in an IR scene generated by SensorVision.